Non-parametric mass modeling of gravitational lenses: implication for the Hubble parameter estimation

B. Mihov, L. Slavcheva-Mihova
Institute of Astronomy and NAO, Bulgarian Academy of Sciences, Sofia, Bulgaria

Abstract. The strong gravitational lensing provides us with an independent estimate of the Hubble parameter, H_0, given the time delay between the images and the mass model of the lens. The rise of the number of lensed systems used to derive H_0 reduces the mass model degeneracies and results in the precise determination of the global value of H_0. The accuracy of the observational constraints is of importance for building a reliable lens mass model. We select a sample of lens systems with available time delay estimates. The most recent values of the time delays (e.g., obtained in the course of COSMOGRAIL programme), positions, and redshifts are compiled. For the sake of increasing the number of observational constraints, quadruple imaged lens systems are chosen. The mass profile is determined using non-parametric modeling. As a result we obtain estimates of the Hubble parameter and of the slope of the lens mass profile. In particular, the radial density profiles are found to be shallower than R^{-2}.

1. Introduction

The strong gravitational lensing provides us with an independent estimate of the Hubble parameter, H0, given the time delay between the images and the mass model of the lens. The rise of the number of lensed systems used to derive H_0 reduces the mass model degeneracies and results in the precise determination of the global value of H_0. The accuracy of the observational constraints is of importance for building a reliable lens mass model. We select a sample of lens systems with available time delay estimates. The most recent values of the time delays (e.g., obtained in the course of COSMOGRAIL programme), positions, and redshifts are compiled. For the sake of increasing the number of observational constraints, quadruple imaged lens systems are preferably chosen. The mass profile is determined using non-parametric modeling. As a result we obtain ensemble estimates of the Hubble parameter and of the slope of the lens mass profile. For this study we selected 3 quadruple and 4 double gravitationally lensed systems.

2. Modeling strategy

We compiled a list of lenses (both quads and doubles) for which precise estimate of the time delay exists. For the lenses chosen we also searched the literature for the best determination of the redshifts, astrometry, and galaxy light distribution orientation.
The non-parametric modeling was done by means of PixeLens software (version 2.17, Saha and Williams 2004). The mass models are symmetric with *pixrad* parameter of 10. An exception from the symmetry is SDSS J1206+4332, where the lens could be involved in interaction with the nearby galaxy group. If there is a companion galaxy to the main lens we add a point mass. The maximal allowed area, covered by the point mass Einstein radius, is assumed to be 15 arcsec^2, which is a reasonable value for the galaxy scale lenses. We run 100 models for each lens and for the ensemble of lenses. Before running the ensemble modeling we examine the systems case by case to determine the best configuration in each individual case.

3. Results

3.1. Quads

DES J0408–5354. This quad was found by Lin et al. (2017) in the course of the Dark Energy Survey. They measured the redshifts to be z_S = 2.375 and z_L = 0.597. The astrometry and the lens light distribution parameters are taken from Shajib et al. (2018). The interesting thing in this system is that the C image is strongly dimmed by a foreground galaxy with position very close to that of the image. By reason of this the time delays, estimated by Courbin et al. (2017), do not include the C image. The galaxy G2, which is very close to the C image was modeled by a point mass 0.3 arcsec to the E from the image. We were able to predict dt(BC) and dt(CD) as follows: dt(BC) = 7.0 (+1.0/–1.2) days and dt(CD) = 16.0 (+4.7/–7.3) days at 68% confidence. Using the relation dt(i,k) = dt(i,j) + dt(j,k) one could see that our predictions agree to within the uncertainties with delays dt(AD) and dt(BD) as estimated by Courbin et al. (2017): dt(AD) = –155.5 ± 12.8 days and dt(BD) = –42.4 ± 17.6 days. The mass and light distributions are in good agreement; the radial mass profile runs as $R^{-0.88}$. Our estimate of H_0 is 96.6 (+21.5/–22.5) km/s/Mpc.

PG 1115+080. This is the second lensed quasar discovered (Weymann et al. 1980, z_S = 1.722). It is a quadruple fold system. Redshift of the galaxy, z_L = 0.3098, is taken from Tonry et al. (1998). The most recent astrometry was presented by Morgan et al. (2008) and it is based on the HST observations. The time delays in the system were determined by several groups but the most recent and precise are these of Bonvin et al. (2018): dt(AB) = 8.3 (+1.5/–1.6) days and dt(AC) = 9.9 (+1.1/–1.1) days. The lens galaxy is a part of a small group. The largest galaxy is at about 25 arcsec to the SW from the system; we modeled this galaxy as a point mass. We predicted the time delay between A1 and A2 lensed images to be 0.29 (+0.17/–0.04) days. The radial mass profile runs as $R^{-0.97}$. Our modeling resulted in Hubble parameter of 72.4 (+8.4/–27.0) km/s/Mpc.

WFI 2033–4723. This quadruple system was discovered by Morgan et al. (2004). The lens redshift is z_L = 0.6575 ± 0.0002 (Sluse et al. 2019) and the source one is z_S = 1.66044 ± 0.00016 (Momcheva et al. 2015). The astrometry was taken from Vuissoz et al. (2008). The time delays between the BCD images obtained so far are in agreement to each other. Bonvin et al. (2019) were able to obtain a separate light curves of A1 and A2 images that allows them to measure the time delays not relative to the composite A (=A1+A2) image, but to the images A1 and A2 itself, i.e., dt(A1B) and dt(A2C). Regarding dt(A1A2) there is some controversy: Morgan et al. (2018) claim that A1 leads A2 by 3.9 days, whereas Bonvin et al. (2019) find the opposite: A2 leads A1 by a day. We tested both variants. In the case A2 leading A1, however, we got an arrival-time surface with critical points in locations not occupied by the A1 and A2 images. So, we assume A1 to lead A2. We then run PixeLens twice. Initially, we set dt(A1A2) = 0 and as a result we predicted the A1A2 time delay of 3.0 (+0.7/–0.7) days at 68% confidence. Then we used the value of 3.9 days for the final run. Orientation and ellipticity of the light (see Vuissoz et al. 2008, PA of 27.8^0) distributions are matched very well. The radial mass profile runs as $R^{-0.96}$. We got H_0 = 79.5 (+11.5/–21.9) km/s/Mpc.

3.2. Doublets

SDSS J1001+5027. This double system was identified by Oguri et al. (2005) with z_S = 1.838. Later on Inada et al. (2012) reported the lens redshift to be z_L = 0.415. We took the time delay estimates from Rathna Kumar et al. (2013). We used astrometry and galaxy morphological parameters from Rusu et al. (2016). We attribute the differences between the astrometry of Rusu et al. (2016) and that of Oguri et al. (2005) to the lower data resolution of the later authors; see the discussion in Rusu et al. (2016) about this topic. We also modeled the galaxy G2 (see Rusu et al. 2016) as a point mass. The mass model we got has somewhat different orientation compared to the light distribution: our model is elongated to

the NW whereas Rusu et al. (2016) found nearly circular distribution with PA~0^0. The radial mass profile runs as $R^{-0.96}$. We got H_0 = 78.9 (+26.3/–35.4) km/s/Mpc.

SDSS J1206+4332. This double system was identified by Oguri et al. (2005) with z_S = 1.789. The lens redshift given by Oguri et al. (2005) was then improved by Agnello et al. (2016): z_L = 0.745. The time delay was taken from Birrer et al. (2019). Regarding the system astrometry there is some disagreement between the results of Oguri et al. (2005) and Eulares et al. (2013) mainly because of the low resolution of their data. By reason of this we did our own astrometry using a HST frame obtained with the WFC3 camera, IR channel (filter F160W, exposure time 469.167 sec, PID: 1424, PI: T. Treu). The measurements were performed onto the derotated frame (to do that we apply the ORIENTATION keyword) using the MIDAS package: we measured the image and galaxy positions by means of fitting a Gaussian to the marginal distributions in both the *x*- and *y*-directions (CENTER/GAUSS command applied within a square of 8 px size). The image positions obtained with respect to the lensing galaxy are (the images are arival time ordered): dRA(A) = 0.545 ± 0.008 arcsec, dDec(A) = –1.807 ± 0.006 arcsec, dRA(B) = 0.522 ± 0.008 arcsec, dDec(B) = 1.219 ± 0.006 arcsec. We model the clump G1 as a point mass situated 0.882 arcsec exactly to the N of the main. In addition we used asymmetric model because the lens could be involved in interaction with the galaxy group to the N-NW – the tidal arm related to the largest group galaxy supports this claim. The ellipticity and PA of our mass models are in agreement with the same parameters of the lens light distribution obtained via photometric decomposition (Agnello et al. 2016, PA of -38.76^0). We observed a mass excess in the opposite direction to the galaxy group. This could mean that indeed the lensing galaxy interacts with the galaxy group. The radial mass profile runs as $R^{-1.51}$ and the Hubble parameter value is 96.8 (+31.5/–33.5) km/s/Mpc at 68% confidence.

SDSS J1515+1511. This doublet was found by Inada et al. (2014). Redshifts are taken from Shalyapin et al. (2017): z_L = 0.742 and z_S = 2.049. In addition, Shalyapin et al. (2017) derived the time delay to be 211 ± 5 days (A leads B). The system astrometry and lens morphology comes from Rusu et al. (2016). The lens seems to be an edge-on galaxy having a PA of -17.1^0. Our mass distribution, however, has PA of about 75^0-80^0. The radial mass profile runs as $R^{-0.93}$. We got the Hubble parameter of 55.1 (+24.4/–18.6) km/s/Mpc.

UM673. This object was discovered by Macalpine & Feldman (1982) as a z_S = 2.719 quasar. Later on the object was identified as a double lens system by Surdej et al. (1987). The redshift of the galaxy was found to be z_L = 0.491. The time delay comes from Koptelova et al. (2012), astrometry – from CASTLES project, and the galaxy morphology – from Koptelova et al. (2014). We modeled the galaxy G1 as a point mass taking the galaxy astrometry from Koptelova et al. (2014). The resulting mass distribution has somewhat larger PA than the light one – we got PA~60^0 vs. ~30^0 from Koptelova et al. (2014). The PA of the lens models presented by Koptelova et al. (2014), however, agree with ours. The mass profile runs as $R^{-1.08}$. The H_0 parameter is 80.3 (+36.7/–25.6) km/s/Mpc.

3.3 Ensemble

Our run of PixeLens in ensemble mode on all 7 lensed systems resulted in Hubble parameter of 78.4 (+10.3/–9.6) km/s/Mpc. The distribution of the Hubble parameters over 100 models is shown in Fig. 1 along with a Gaussian fit. Our value is in agreement with H_0 = 68.1 ± 5.9 km/s/Mpc obtained by Kumar et al. (2015) for 10 lenses in a similar to ours way, but we have the advantage to use more recent data. Recently, Birrer et al. (2019) obtained 72.5 (+2.1/–2.3) km/s/Mpc using four lenses.

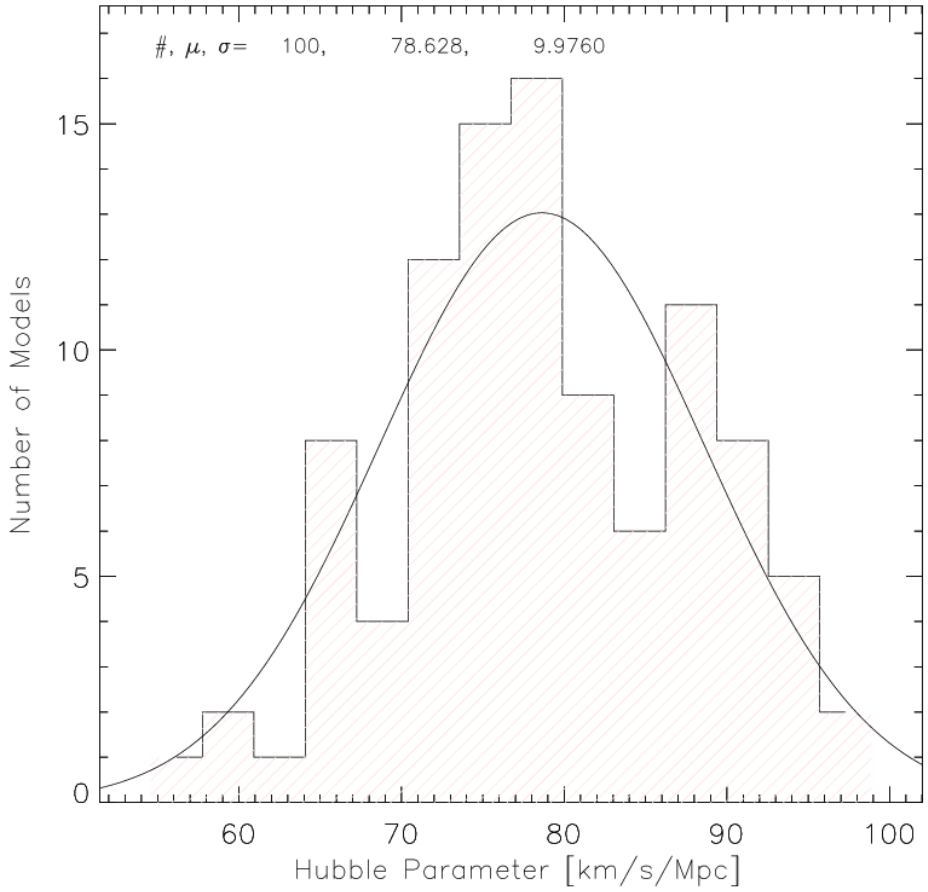

Fig. 1: Hubble parameter distribution. The fitted Gaussians, together with the number of runs and the Gaussian mean and sigma are listed in each plot.

The mass and steepness index distributions are shown in Figs. 2-15; the steepness index is defined as $\Sigma(R) \sim R^{-(\text{steepness index})}$, where Σ is the surface mass distribution. We list in the Table the individual estimates of the steepness index for the each system. The steepness index was found to be less than 2, i.e., the radial density profiles are shallower than R^{-2}.

System	Percentiles of the steepness index		
	16%	50% (median)	85%
DES J0408–5354	0.57	0.70	0.95
PG 1115+080	0.84	1.00	1.34
WFI J2033–4723	0.79	0.94	1.08
SDSS J1001+5027	0.78	1.03	1.39
SDSS J1206+4332	1.29	1.53	1.97
SDSS J1515+1511	1.32	1.55	2.18
UM 673	0.88	1.07	1.54

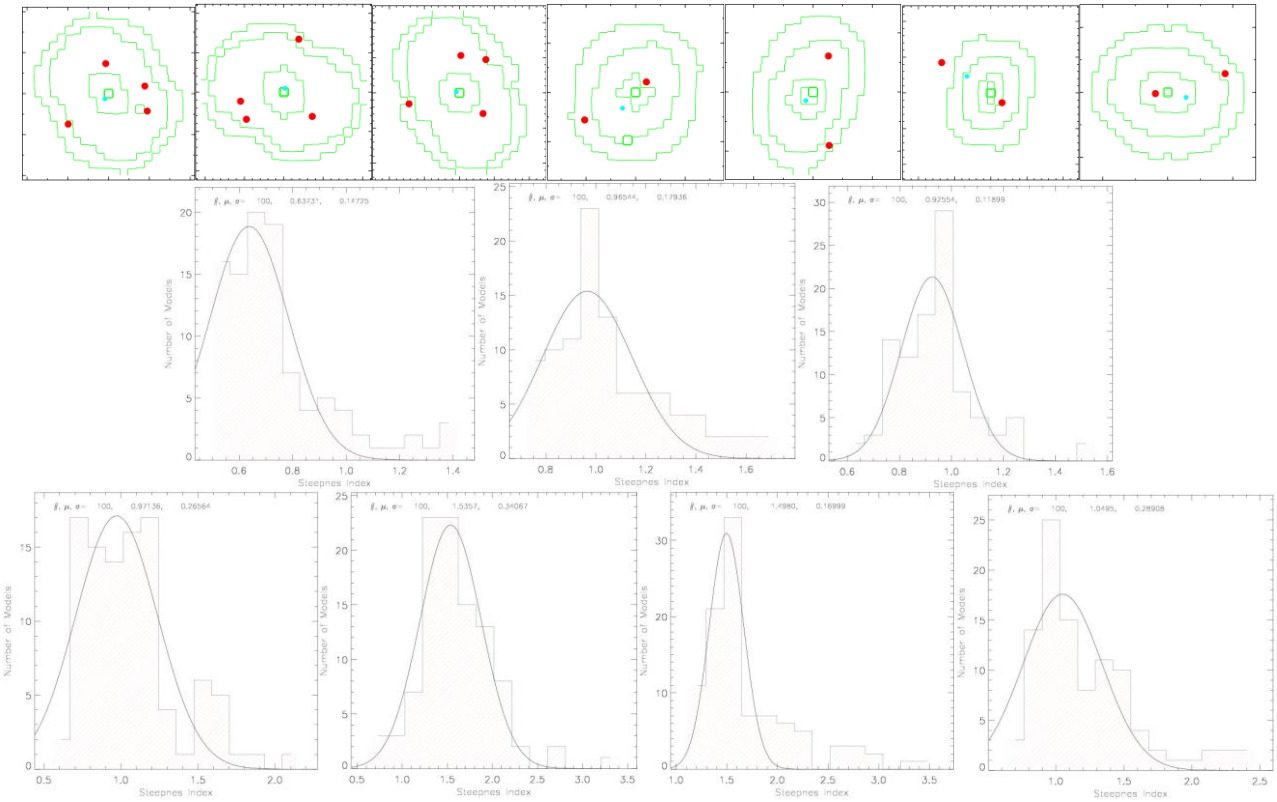

Fig. 2-15: *Mass and steepnes index distributions for the lenses modeled. The fitted Gaussians, together with the number of runs and the Gaussian mean and sigma are listed in each plot.*

Acknowledgements and References

This research is based on activities partially supported by the Bulgarian National Science Fund under contract DN 18/13-12.12.2017.

Agnello et al. 2016, MNRAS, 458, 3830

Birrer et al. 2019, MNRAS, 484, 4726

Bonvin et al. 2018, A&A, 616, A183

Bonvin et al. 2019, arXiv:190508260

Courbin et al., 2018, A&A, 609, A71

Eigenbrod et al. 2007, A&A, 465, 51

Eulaers et al. 2013, A&A, 553, A121

Inada et al. 2012, AJ, 143, 119

Inada et al. 2014, AJ, 147, 153

Koptelova et al. 2012, A&A, 544, A51

Koptelova et al. 2014, A&A, 566, A36

Kumar et al. 2013, A&A, 557, A44

Kumar et al. 2015, A&A, 580, A38

Lin et al. 2017, ApJL, 838, L15

MacAlpine, G. M., Feldman, F. R., 1982, ApJ, 261, 412

Momcheva et al. 2015, ApJS, 219, 29

Morgan et al. 2004, AJ, 127, 2617

Morgan et al. 2008, ApJ, 689, 755

Morgan et al. 2018, ApJ, 869, 106

Oguri et al. 2005, ApJ, 622, 106

Rusu et al. 2016, MNRAS, 458, 2

Rusu et al. 2019, arXiv:190509338

Saha, P., Williams, L. L. R. 2004, ApJ, 127, 2604

Shajib et al., 2019, MNRAS, 483, 5649

Shalyapin et all. 2017, ApJ, 836, 14

Surdej et al. 1987, Nature, 329, 695

Tonry, J. L. 1998, AJ, 115, 1

Vuissoz et al. 2008, A&A, 488, 481

Weymann et al. 1980, Nature, 285, 641